

## Supporting Information

### Diffusion-determined Assembly of All-climate Supercapacitors via Bioinspired Aligned Gel

*Jie Zhou, Chu Wu, Gumi Wei, Junjie Wei, Songyan xi, Ziyang Tai, Saiji  
Shen, Dongbei Wu\*, Qigang Wang\**

#### 1. Materials

3-[Dimethyl-[2-(2-methylprop-2-enoyloxy)ethyl]azaniumyl]propane-1-sulfonate (SBMA,  $M_n = 279$ ), and acrylamide (AAM) were purchased from Sigma-Aldrich Reagent Company. Organic photo-initiator 2, 2-diethoxyacetophenone (DEAP), lithium bis(trifluoromethanesulfonyl)imide (LiTFSI), poly (ethylene glycol) dimethacrylate (PEGMA,  $M_n=200$ ), ethanol, potassium hydroxide (KOH), melamine, formaldehyde, hexamethylenetetramine, and formic acid were purchased from Shanghai Energy Chemical Co., Ltd, Shanghai, China. Acetylene black and polytetrafluoroethylene (PTFE, 60 wt% aqueous dispersion) were obtained from Shanghai 3F New Material (Shanghai) and Aladdin Chemistry Co., Ltd.

#### 2. Synthesis of HPC

N, O co-doped honeycomb carbon electrodes were prepared according to the method described by Song et al.<sup>[1]</sup> First, 6.306 g melamine, 10 mL formaldehyde solution (37 wt%, 0.1 mol), and 0.021 g hexamethylenetetramine were dissolved in 120 ml of water. The mixture was heated to 65 °C under stirring to yield a transparent solution. Then,

0.70 g SiO<sub>2</sub> and 0.1 mL formic acid were successively added and the solution was stirred for 3 h. Finally, after carbonization, HF solution was used to etch the SiO<sub>2</sub>@polymer, and the resultant carbons were activated. The HPC electrode was soaked in 5M LiTFSI for 48h.<sup>[1]</sup>

### **3. Preparation of non-aligned gel, aligned gel and normal gel**

Typically, the precursors consisted of 1 wt% DEAP and 1 wt% PEGMA, as well as 25.0, 22.0, 19.0, 16.0, or 13.0 wt% AAM, and corresponding zwitterionic SBMA monomer concentrations of 0.0, 3.0, 6.0, 9.0, 12.0 wt% SBMA, respectively. Then, precursor solutions were injected into glass tubes with a diameter of 14 mm, and then they were directional frozen over liquid N<sub>2</sub> at the rate of 2 mm/min by using tensile-compressive tester. Afterwards, the aligned gels were obtained *via* UV cryopolymerization (Shanghai Huijun Science & Technology Development Co., Ltd, 99.8 mW/cm<sup>2</sup>, 365 nm) for 4 hours in a -18 °C refrigerator. Afterwards, the as-prepared samples were freeze-dried for 72 h. The non-aligned aerogels with same precursor contents were obtained *via* polymerization in room temperature after freeze-dried process for 72 h. The normal aerogels with same precursor contents were obtained after they were polymerized in room temperature, followed by ambient pressure drying process. Aligned gels, non-aligned gels, and normal gels were obtained after these above-mentioned aerogels were soaked into 5M LiTFSI solution, prior to swelling measurement and peeling test.

### **4. Fabrication of AGS-9%, AGS, CSS, N-AGS-9%**

The AGS-9% and N-AGS-9% precursors consisted of 1 wt% DEAP and 1 wt%

PEGMA, as well as 16.0 AAM, and zwitterionic SBMA monomer 9.0 wt% SBMA.

AGS-9% aerogels were obtained *via* directional frozen, UV cryopolymerization and freeze-drying. N-AGS-9% aerogels were obtained *via* freeze-drying. Similar, The AGS precursors consisted of 1 wt% DEAP and 1 wt% PEGMA, as well as 25.0 AAM, and zwitterionic SBMA monomer 0.0 wt% SBMA. AGS aerogels were obtained *via* directional frozen, UV cryopolymerization and freeze-drying. Finally, these aerogels were rinsed 10 times with 2.5M LiTFSI solution to remove of unreacted chemicals, followed by soaking in the high concentration of 5M LiTFSI for at least 2 days. To obtain neutrally swollen gel electrolytes, the volume of the 5M LiTFSI solution is 500 times larger than that of aerogels. For a comparative experiment, CSS utilized separators soaked in 5LiTFSI for at least 2 days as electrolyte.

## **5. Pre-treatments and characterizations**

### **5.1 Swelling properties**

The as-prepared hydrogels were freeze-dried for 72 h. Swelling rates were measured by weighing the samples after immersion in highly concentrated LiTFSi solutions for varying durations of time. Swollen gel mass ( $m_w$ , g) was recorded directly after wiping off excess water. The swelling ratio (SR) was calculated as:  $SR (\%) = (m_w - m_d)/m_d$ , where  $m_w$  and  $m_d$  were the masses of the samples in the swollen or dried conditions.

### **5.2 Pre-treatment of SEM samples**

The samples (3 mm × 3 mm × 3 mm) were rapidly quenched with liquid nitrogen, and then freeze-dried (Scientz-10N, Ningbo, China) for 48 h. A thin layer of gold (about 4 nm) was sputter-coated onto the samples before they were scanned with a field emission SEM (Hitachi S-4800, JEOL, Tokyo, Japan) at an accelerating voltage of 5 kV.

### **5.3 Compression experiments**

Gels were measured by a universal tensile-compressive tester (CMT 6503, SANS, China) using the GB/T 1040.3-2006 Standard. Cylindrical samples were tested at a strain rate of 5 mm min<sup>-1</sup>. The Young's modulus was extracted from the initial linear region of the stress-strain curve. All results are the average of three independent experiments.

### **5.4 Peeling experiments**

The interfacial toughness between the gel and the solid substrates was measured via 90 ° peeling tests setup at the crosshead speed of 50 mm/min (Farui Co., China). Gels were measured in a size of 20 mm × 100 mm × 3 mm. As a stiff backing for the gel sheet, the plastic paper was adhered on the top of gel.

### **5.5 Brunauer – Emmett – Teller (BET) measurements**

The nitrogen adsorption–desorption isotherms of HPC were obtained at –196 °C by an automatic adsorption instrument (ASAP 2460, Micromeritics). The average pore diameters and specific surface areas were computed according to the Brunauer–Emmett–Teller (BET) equation. Additionally, the pore size distribution was derived from the density functional theory (DFT) method.

### **5.6 Thermogravimetric analysis (TGA) and Differential Scanning calorimetry (DSC) measurements**

The samples with a mass of 5 mg was put in a sealed in aluminum oxide pans. The experiments were conducted using a DISCOVER TGA550 and DSC2500 (10 °C/min) under N<sub>2</sub> over a temperature range from -196 to 200 °C.

### **5.7 Raman spectroscopy measurements**

Raman spectrum was collected using a Horiba modular Raman system with a diode laser source (wave length 514 nm).

### **5.8 X-ray photoelectron spectroscopy (XPS) measurements**

The surface chemical properties of HPC were investigated by XPS with monochromatic Al Ka as the radiation source.

### **5.9 X-ray diffraction (XRD) measurements**

XRD patterns were recorded using a Bruker Advance X-ray diffractometer-AXS (D8-Advance, Germany) equipped with a monochromator using Cu Ka radiation ( $\lambda = 1.54 \text{ \AA}$ ).

### **5.10 LF-NMR measurements**

The relaxation time ( $T_2$ ) of sample was obtained by Nuclear magnetic resonance analyzer (PQ001-20-025, Suzhou Niumag Analytical Instrument Co., China).

### **5.11 Rheological analysis**

Rheological tests of samples (cylinders, 20 mm in diameter and 2 mm in height) were carried out by using a Thermo Haake RS6000 rheometer (Thermo Scientific) at the room temperature.

### **5.12 Characterization of solid state supercapacitors**

AC impedance measurements were measured ionic conductivity. The electrolytes were SS/electrolyte/SS (SS: stainless steel electrode) sandwiched structured coupled with a polytetrafluoroethylene (PTFE) clamp which can ensure circuit in good contact. AC impendence measurements with an amplitude of 10 mV was carried out in the

frequency range from 1000 Hz to 0.01Hz. The conductivity of the electrolyte is calculated according to the equation (1)

$$\sigma = \frac{l}{ARb} \quad (1)$$

Where  $Rb$  is the resistance of the bulk electrolyte,  $l$  is the thickness of the gel and  $A$  is the area of electrode covered by gel.

The electrochemical capacitance ( $F\ g^{-1}$ ) of the supercapacitor can be calculated from the galvanostatic charge–discharge curves, according to the equation (2)

$$C_s = \frac{4I\Delta t}{m\Delta U} \quad (2)$$

Where  $I$  is the discharge current,  $\Delta t$  is the discharge time,  $m$  is the total active material mass on two electrode,  $\Delta U$  is the voltage after  $IR$  drop. <sup>[2]</sup>

The energy density ( $E$ , Wh  $kg^{-1}$ ) and power density ( $P$ , W  $kg^{-1}$ ) are obtained based on following forms (3) and (4):

$$E = \frac{C_s \Delta U^2}{8} \quad (3)$$

$$P = \frac{E}{\Delta t} \quad (4)$$

Where  $C_s$  is the capacitance ( $F\ g^{-1}$ ),  $\Delta U$  is the voltage (V) after  $IR$  drop and  $\Delta t$  is the discharge time (s).<sup>[3]</sup>

## 6 Figures.

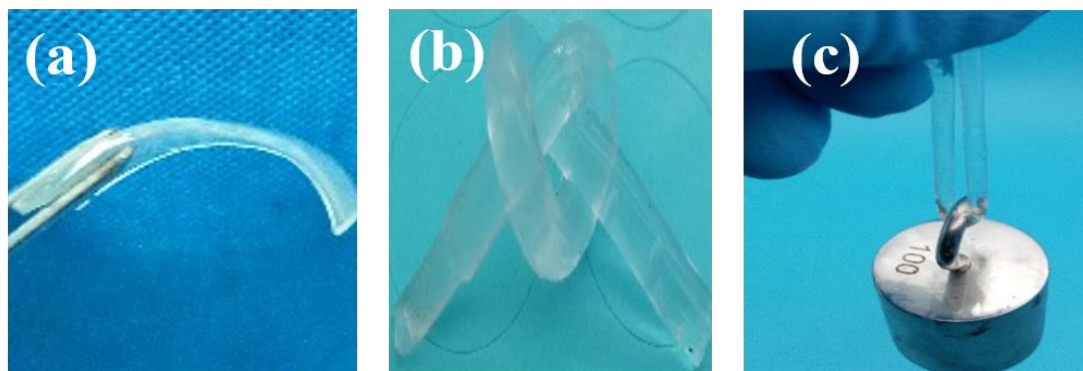


**Fig. S1.** (a-c) Images of the flexible gel.

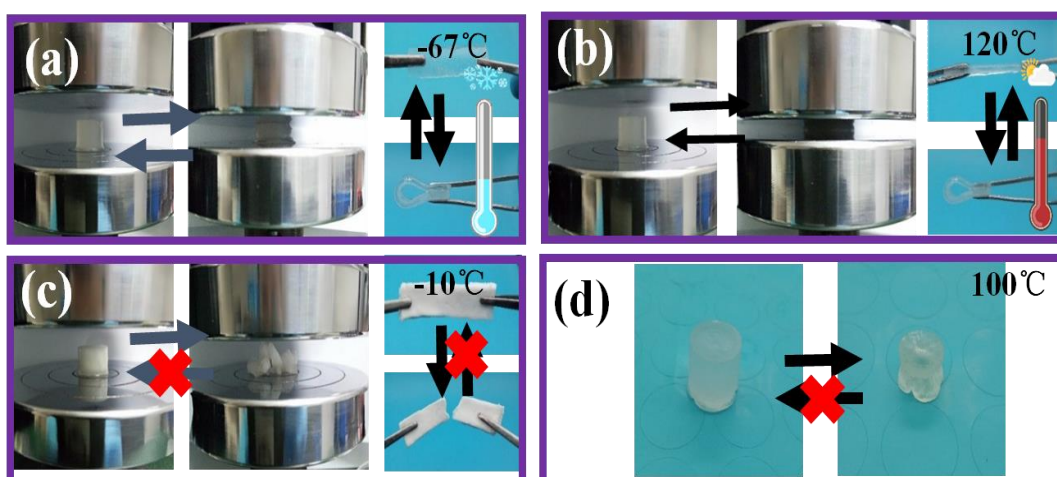


**Fig. S2.** The gel maintained nearly all of its elasticity at both (a)  $-67^{\circ}\text{C}$  and (b)  $120^{\circ}\text{C}$ . (c) The hydrogel turned into an ice-like solid state that could easily be broken at  $-10^{\circ}\text{C}$ . (d) The hydrogel rapidly dehydrated into a rigid and shrunken solid when heated to  $100^{\circ}\text{C}$ .

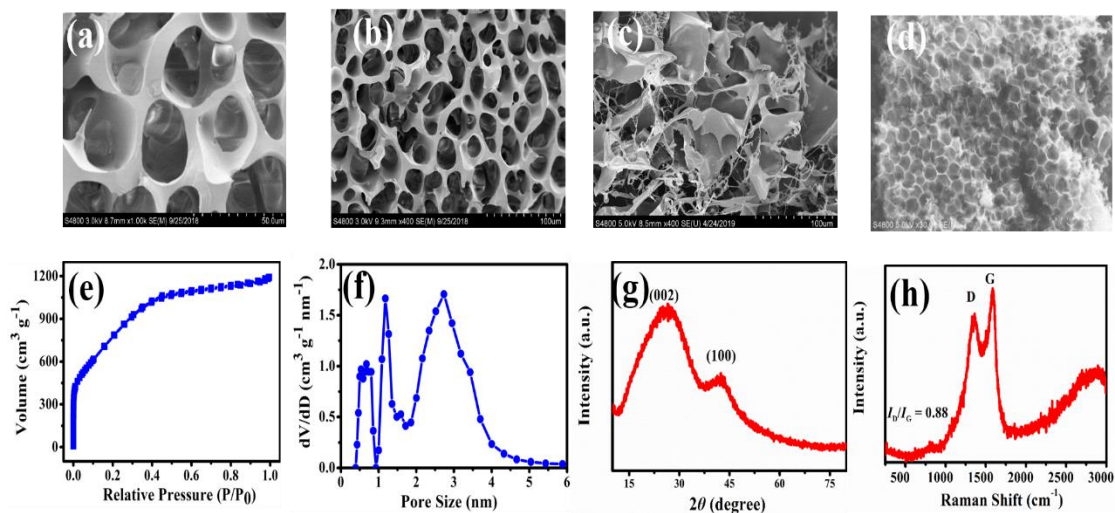


**Fig. S3.** (a, b) SEM images of the aligned gel cross section. (c) SEM images of the non-aligned porous structure of gel. (d) SEM image of HPC. (e) N2 adsorption/desorption isotherms of HPC. (f) Pore size distribution curves of the HPC. (g, h) XRD and Raman spectra patterns of the HPC.

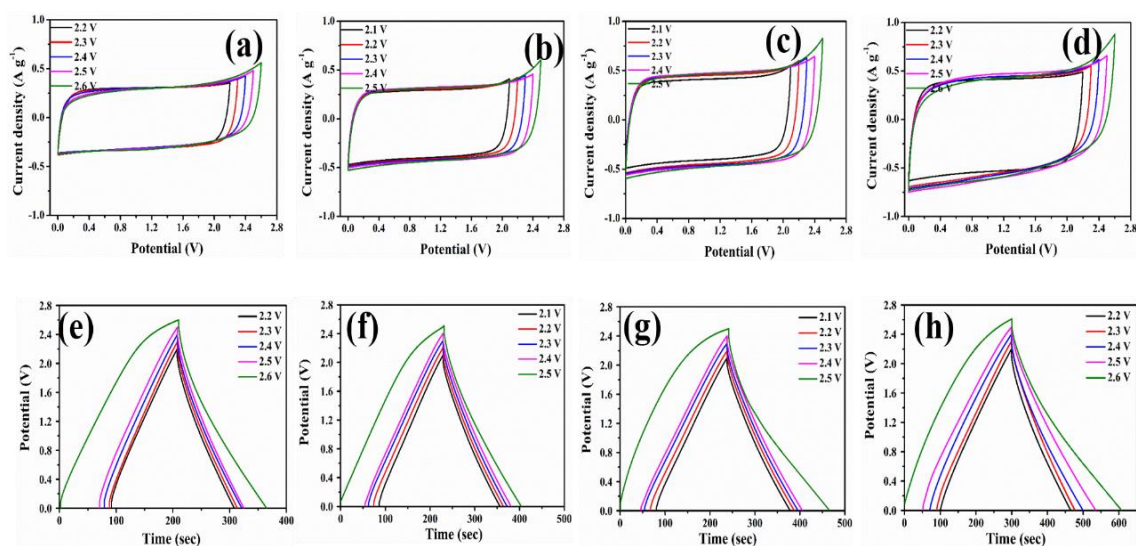


**Fig. S4.** (a-d) CV curves of the N-AGS-9%, CSS, AGS and AGS-9% with different cut-off voltages. (e-h) GCD curves of the N-AGS-9%, CSS, AGS, and AGS-9% with different cut-off voltages.



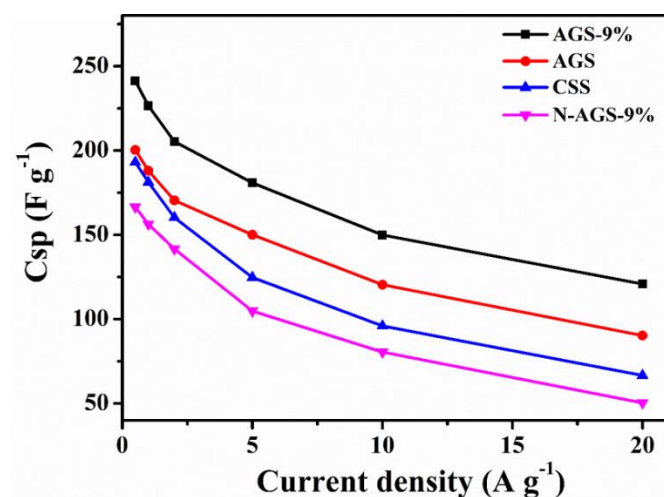


**Fig. S5.** Comparison of  $C_{sp}$  of different gel structures as a function of current density

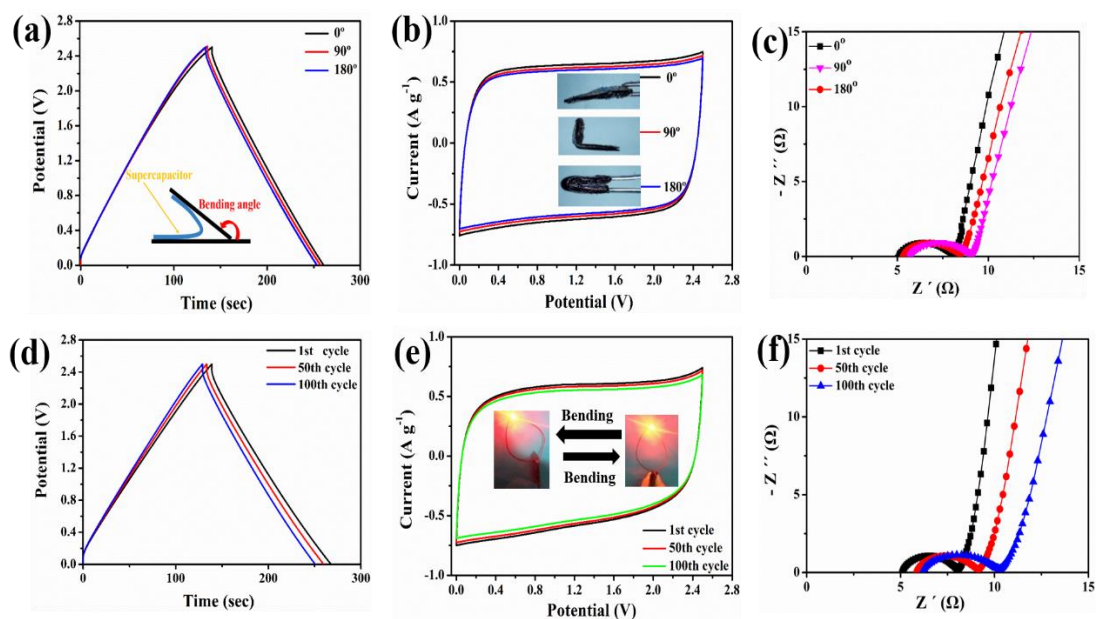


**Fig. S6.** (a) The GCD curves at various bending angles. (b) The CV curves at various bending angles. (c) The EIS curves at various bending angles. (d) The GCD curves at various cycling bending process for 180°. The inset shows images of the device bent at various angles. (e) The CV curves at various cycling bending process for 180°. (f) The EIS curves at various cycling bending process for 180°.

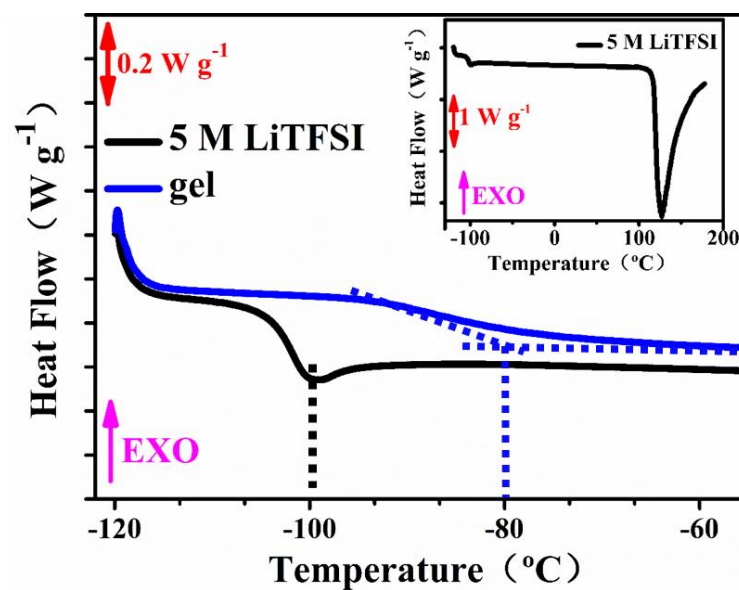


**Fig. S7.** DSC traces from -120 to -55°C of the 5 M LiTFSI and gel. Inset: DSC traces of the 5M LiTFSI from 80 to 145°C.

## 7 Table

**Table S1.** Performance comparisons of the prepared devices and other devices.

Electrolyte	Electrode	Csp (F g <sup>-1</sup> )	ESPW (V)	T (°C)	E (Wh kg <sup>-1</sup> )	Ref.
Organic liquid	ACs <sup>a)</sup>	177(5mV s <sup>-1</sup> )	2.5	-100-60	38.4	6
	AC <sup>b)</sup>	NM <sup>c)</sup>	2.3	-55	NM <sup>c)</sup>	7
Ionic liquid/gel	AC <sup>b)</sup>	176(1A g <sup>-1</sup> )	2.5	25-200	38.2	15
	AC <sup>b)</sup>	174(1A g <sup>-1</sup> )	1.0	RT	6.0	18
Aqueous solution/ based	Carbon Monoliths	143(2A g <sup>-1</sup> )	2.4	RT	24	27
	AC <sup>b)</sup>	108(1A g <sup>-1</sup> )	2.2	-30-50	18.15	35
	MnO <sub>2</sub> - based	239(2mV s <sup>-1</sup> )	1.4	RT	16.3	36

<b>gel</b>	CAPs <sup>d)</sup>	233(1A g <sup>-1</sup> )	1.0	RT	23	37
	CCNP <sup>e)</sup>	190(1A g <sup>-1</sup> )	3.0	RT	59.4	38
<b>Aligned gel</b>	<b>HCP</b>	<b>241(0.5A g<sup>-1</sup>)</b>	<b>2.5</b>	<b>-56-100</b>	<b>52.3</b>	<b>This Work</b>

Csp: specific capacitance;

ESPW: electrochemically stable potential window;

T: temperature-tolerant;

E: energy density

a) a bimodal distribution of micropores and mesopores, and with predominantly slit-shaped pores

b) commercial activated carbon

c) not mentioned in the paper

d) conjugated aromatic polymers

e) continuous carbon nitride polyhedron

## 7. Reference

[1] Z. Song, L. Li, D. Zhu, L. Miao, H. Duan, Z. Wang, W. Xiong, Y. Lv, M. Liu, L.

Gan, *J. Mater. Chem. A* **2019**, 7, 816-826.

[2] Yang, P. H.; Mai, W. J., *Nano Energy* **2014**, 8, 274-290.

[3] Kang, Y. J.; Chun, S. J.; Lee, S. S.; Kim, B. Y.; Kim, J. H.; Chung, H.; Lee, S. Y.;

Kim, W., *ACS Nano* **2012**, 6 (7), 6400-6406.